# ION MOVEMENT THROUGH GRAMICIDIN A CHANNELS

## Interfacial Polarization Effects on Single-Channel Current Measurements

OLAF SPARRE ANDERSEN
*Department of Physiology and Biophysics, Cornell University Medical Center, New York, New York 10021*

ABSTRACT Gramicidin A single-channel current-voltage characteristics were studied at low permeant ion concentrations and very high applied potentials. The purpose of these experiments was to elucidate the basis for the small, but definite, voltage dependence observed under these circumstances. It was found that this residual voltage dependence is a reflection of interfacial polarization effects, similar to those proposed by Walz et al. (*Biophys. J.* 9:1150–1159). It will be concluded that there exists an effectively voltage-independent step in the association reaction between a gramicidin A channel and the permeating ion. Some consequences of interfacial polarization effects for the analysis of conductance vs. activity relations will be discussed.

## INTRODUCTION

Gramicidin A single-channel current-voltage characteristics, measured at low salt concentrations and very high potentials, exhibit a small, but finite, voltage dependence (Andersen, 1983 *a*). This voltage dependence could, in principle, reflect some intrinsic property of the channel, or it could be the result of the unavoidable changes in interfacial ion concentrations that are associated with the application of a potential difference across a lipid bilayer membrane (Everitt and Haydon, 1968; Walz et al., 1969). The purpose of this article is to examine this question. It will be shown that this residual voltage dependence is indeed the result of the interfacial polarization associated with the applied potential.

## THEORY

A complete analysis of interfacial polarization effects on diffusion-controlled currents through membrane-bound channels is difficult. It is necessary to consider not only the complex electrostatics of a membrane-bound channel (Levitt, 1978), but also the stationary (but nonequilibrium) ion distribution in the aqueous interfacial regions. No attempt will be made to deal with these problems in detail. Instead I will present an approximate treatment of interfacial polarization effects on single-channel currents. This treatment is deficient in some respects, but it has the distinct advantage that it leads to analytical expressions for the "distortions" in the currents.

The first section presents the electrostatic model, while the second section focuses on interfacial polarization effects at high potentials where aqueous diffusion limitations will be particularly important. An analysis of interfacial polarization effects at arbitrary potentials is given in the Appendix.

The research for this paper was done with the technical assistance of Frank Navetta.

### The Electrostatic Model

A cation-selective channel is assumed to be incorporated into a planar lipid bilayer that carries no net charge. The membrane separates symmetrical aqueous phases containing the univalent salt of a permeant cation. The aqueous phases may, in addition, contain equal concentrations of an inert (impermeant and nonblocking) uni-univalent electrolyte. The concentration of the permeant ion is denoted by $c$, the concentration of the impermeant cation is $c_t - c$. The ionic strength of the aqueous phases is thus equal to $c_t$. The length of the channel is assumed to equal the thickness of the hydrocarbon core of the bilayer, which extends from $x = 0$ to $x = d$. It is assumed that the electrostatic field, due to the applied potential, is constant within the membrane. It is further assumed that the dielectric characteristics of the channel and surrounding membrane can be approximated by those of a uniform disk, with lateral dimensions sufficiently large to permit the aqueous interfacial regions to be treated as one-dimensional structures.[1] The specific capacitance of this disk is $C_m^* = \epsilon_o \cdot \epsilon_r^{m*}/d$, where $\epsilon_o$ is the capacitance of free space and $\epsilon_r^{m*}$ is the effective dielectric constant of the disk.

When no potential difference is applied across the membrane, the ion concentrations are assumed to be uniform throughout the aqueous phases. (Complications that might arise from multiple ion occupancy are thus ignored; this assumption is justified in Finkelstein and Andersen, 1981.) It is further assumed that the concentration and potential profiles in the aqueous diffuse layers can be described by the Boltzmann and Poisson equations:

$$c^+(x) = c \cdot \exp[-e \cdot \Delta V(x)/kT] \qquad (1\,a)$$

$$c^-(x) = c \cdot \exp[e \cdot \Delta V(x)/kT] \qquad (1\,b)$$

[1] This assumption is certainly incorrect in detail. It is retained, because it leads to a considerable simplification of development of the model, while it retains the essential physical feature: that the application of a potential difference across a channel polarizes the aqueous solutions at the channel entrances. Note that there are two separate aspects to this assumption. The first concerns the proportionality between the transmembrane potential and the extent of the interfacial polarization, this can be justified at potentials sufficiently low that the superposition principle (of fields) apply. The second aspect concerns the invariance of $C_m^*$ with changes in ionic strength, this is harder to justify.

and

$$\frac{d^2\Delta V(x)}{dx^2} = -\frac{\rho(x)}{\epsilon_0 \cdot \epsilon_r^{H_2O}} \tag{2a}$$

$$= -\frac{F \cdot [c^+(x) - c^-(x)]}{\epsilon_0 \cdot \epsilon_r^{H_2O}} \tag{2b}$$

where $c^+$ and $c^-$ denote the concentrations of cations and anions, respectively, and

$$\Delta V(x) = V(x) - V(-\infty), \qquad x \leq 0 \tag{3 a}$$

$$\Delta V(x) = V(x) - V(\infty), \qquad d \leq x. \tag{3 b}$$

$V(x)$ denotes the potential (as a function $x$), $e$ is the elementary charge, $k$ is Boltzmann's constant, $T$ is temperature in Kelvin, $\rho$ is the aqueous space charge density, $\epsilon_r^{H_2O}$ is the dielectric constant of the aqueous phase, and $F$ is Faraday's constant.

The boundary conditions, at $x = 0$ and $x = d$, are

$$\epsilon_r^{m*} \cdot \frac{dV_m}{dx} = \epsilon_r^{H_2O} \cdot \frac{d\Delta V}{dx} \tag{4}$$

or

$$\epsilon_r^{m*} \cdot \frac{\Delta V_m}{d} = \epsilon_r^{H_2O} \cdot \frac{d\Delta V}{dx} \tag{5}$$

where $V_m$ denotes the potential within the membrane and $\Delta V_m$ is the potential difference that falls across the membrane itself. The partitioning of the applied potential difference, $V = V(-\infty) - V(\infty)$, between the membrane itself and the two aqueous diffuse layers is (cf. Everitt and Haydon, 1968; and Walz et al., 1969)

$$\Delta V_m \cdot (\epsilon_r^{m*}/d) = (\epsilon_r^{H_2O}/L_D) \cdot (2kT/e) \cdot \sinh(e \cdot \Delta V/2kT) \tag{6}$$

where $L_D$ denotes the Debye length in the aqueous phases,

$$L_D = [\epsilon_o \cdot \epsilon_r^{H_2O} \cdot kT/(2 \cdot F \cdot e \cdot c_t)]^{0.5}, \tag{7}$$

and $\Delta V$ denotes the value of $\Delta V(d)$

$$\Delta V = (V - \Delta V_m)/2. \tag{8}$$

Eq. 6 simplifies considerably when

$$\Delta V < kT/e, \tag{9}$$

in which case it can be rewritten as

$$\Delta V_m \cdot (\epsilon_r^{m*}/d) = \Delta V \cdot (\epsilon_r^{H_2O}/L_D). \tag{10}$$

Relation 9 will be satisfied for all experimental conditions encountered in this article, the remaining analysis will therefore be based upon Eq. 10 rather than 6. The explicit expressions for $V_m$ and $\Delta V$ are now obtained as

$$\Delta V_m = V \cdot (1 - 2\alpha) \tag{11}$$

and

$$\Delta V = V \cdot \alpha, \tag{12}$$

where

$$\alpha = (\epsilon_r^{m*}/d)/(\epsilon_r^{H_2O}/L_D + 2 \cdot \epsilon_r^{m*}/d) \tag{13 a}$$

$$= C_m^*/(\epsilon_o \cdot \epsilon_r^{H_2O}/L_D + 2 \cdot C_m^*). \tag{13 b}$$

(Note that the term $\epsilon_o \cdot \epsilon_r^{H_2O}/L_D$ corresponds to the specific capacitance of the diffuse double layer in the Gouy-Chapman theory of polarized interfaces (Bockriss and Reddy, 1970; Aveyard and Haydon, 1973). But there is no physical correlate to the diffuse double-layer capacitance in the present context, since there is no double layer associated with a single interfacial region; the charge separation is between the two aqueous regions.)

At ionic strengths above 0.01 M, or so, the term $\epsilon_o \cdot \epsilon_r^{H_2O}/L_D$ will be much larger than $C_m^*$, $\alpha$ can then be approximated as

$$\alpha = C_m^* \cdot L_D/(\epsilon_o \cdot \epsilon_r^{H_2O}) \tag{14}$$

or

$$\alpha = kT \cdot 2 \cdot A \cdot C_m^*/(e \cdot \sqrt{c_t}), \tag{15}$$

where

$$A = (8 \cdot N \cdot kT \cdot \epsilon_o \cdot \epsilon_r^{H_2O})^{-0.5} \tag{16}$$

and $N$ is Avagadro's number.

The potential profiles in the aqueous diffuse layers can be expressed, relative to the adjacent bulk aqueous phases, as

$$u(x) = -u_{dl} \cdot \exp(x/L_D), \qquad x \leq 0 \tag{17 a}$$

$$u(x) = u_{dl} \cdot \exp[(d - x)/L_D], \qquad d \leq x \tag{17 b}$$

where the potentials are normalized, $u = eV/kT$, $u_{dl} = e\Delta V/kT$, while the concentration profiles can be evaluated using Eqs. 1 *a*, *b*, 12, and 17 *a*, *b*.

In particular, one can write

$$c^+(0) = c \cdot \exp(\alpha \cdot u) \tag{18 a}$$

$$c^+(d) = c \cdot \exp(-\alpha \cdot u). \tag{18 b}$$

## Interfacial Polarization Effects on Single-Channel Currents at High Potentials

The above expressions implicitly contain the assumption that equilibrium exists in the aqueous double layers. They cannot be exact in the presence of net ion movement through the channel and the adjacent aqueous phases. The distortions in concentration and potential profiles will, however, be insignificant unless net ion movement through the channel is so large that the aqueous convergence permeability becomes a significant factor in limiting the flux. The ion concentrations close to the channel entrances will in this case deviate from the predictions of Eqs. 18 *a*, *b*.

This diffusion-dependent concentration polarization will occur quite close to the channel entrance, as the major concentration changes occur within one capture radius, $r_o$, of the channel entrance (Andersen, manuscript in preparation). From Eqs. 1 *a*, *b*, and 17 *a*, *b* it can thus be inferred that the aqueous double-layer regions will function as essentially infinite aqueous phases vis-a-vis ion movement through the channel as long as

$$r_o < L_D. \tag{19}$$

A reasonable upper estimate for $r_o$ is the luminal channel radius, ~2 Å (Urry, 1972).[2] Eq. 19 should thus be satisfied for ionic strengths up to ~0.5 M. Eq. 19 will therefore be satisfied over the concentration range where interfacial polarization effects are predicted to be significant (Walz et al., 1969). It will, in the following, be assumed that the aqueous

[2]A smaller estimate for $r_o$ was obtained in Andersen (1983 *a*, *b*). This smaller value reflects, however, also factors such as hydrodynamic restrictions on particle diffusion close to the membrane and partition effects of ions between the bulk aqueous phase and the aqueous phase close to the membrane.

double layers behave as infinite reservoirs, such that the bulk phase ion concentrations relevant for ion entry into the channel are given by Eqs. 18 *a*, *b*.[3]

Interfacial polarization effects are particularly important at low permeant ion concentrations and high applied potential, when the current through the channel, $i(u)$, is equal to the rate of ion association with the channel:

$$i(u) = e \cdot k_1(u) \cdot c(0) \tag{20}$$

where $u$ is assumed to be positive and $k_1(u)$ denotes the (voltage-dependent) association rate constant. (The reason for writing the association rate constant this way is that the magnitude of $k_1(u)$ generally will be a function of several, voltage-dependent and -independent, rate constants). To express $i(u)$ as a function of $c$, Eq. 18 *a* is introduced into Eq. 20 to give

$$i(u) = e \cdot k_1(u) \cdot c \cdot \exp(\alpha \cdot u) \tag{21}$$

which can be linearized when Eq. 9 is satisfied:

$$i(u) = e \cdot k_1(u) \cdot c \cdot (1 + \alpha \cdot u). \tag{22}$$

A particularly interesting and important case occurs if there exists a voltage-independent step in the association reaction, a diffusion-controlled step, for example, and the potential is sufficiently high that $k_1(u)$ reaches its upper voltage-independent limit $k_1^*$. The single-channel current can then be written as

$$i(u) = i_{\text{lim}} \cdot (1 + \alpha \cdot u), \tag{23}$$

where

$$i_{\text{lim}} = e \cdot k_1^* \cdot c \tag{24}$$

is the voltage-independent limiting current in the absence of interfacial polarization, as measured in the presence of a very high concentration of inert support electrolyte.

The essential feature of interfacial polarization effects can be appreciated by noting that $\alpha$ varies inversely with the square root of the ionic strength in the aqueous phases (Eq. 15). It was this characteristic property that was utilized in the experimental protocols and subsequent data analysis.

## MATERIALS AND METHODS

All experiments were done as single-channel current measurements on gramicidin A channels in diphytanoylphosphatidylcholine/*n* - decane (DPhPC) membranes at 25°C, using an isolated bilayer patch clamp technique. The procedures and materials were those described in the preceding article (Andersen, 1983 *a*).

## RESULTS

### The Shape of Single-Channel Current-Voltage Characteristics at Different Salt Concentrations and Ionic Strengths

The variations in shape among gramicidin A single-channel current-voltage characteristics at different aqueous CsCl concentrations (0.01 to 0.1 M) are illustrated in Fig. 1. The scale on the ordinate varies with the permeant ion concentration to permit a convenient comparison of the shapes of the curves. Similar results were obtained with KCl, RbCl, and $NH_4Cl$ (data not shown). At 0.1 M CsCl the single-channel currents approach a very weakly volt-

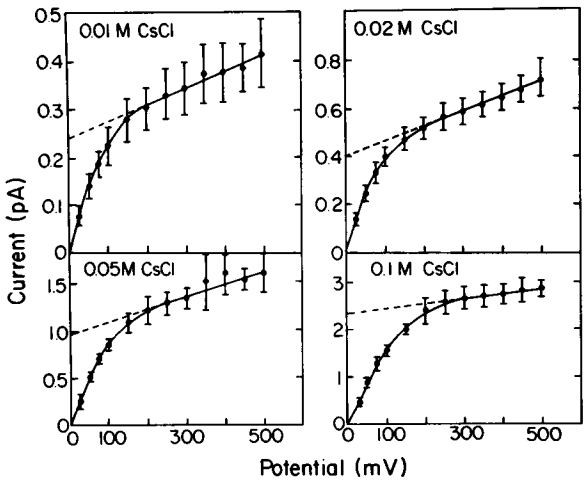


FIGURE 1 Gramicidin A single-channel current-voltage characteristics at different CsCl concentrations. The points indicate mean (± SD) of the amplitude histograms. The straight lines at high potential are regression lines determined by weighted least-squares linear regression according to Eq. 26 from the data indicated by the solid line segments. The interrupted segment denote the extrapolation back to $V = 0$. The solid curves have no theoretical significance.

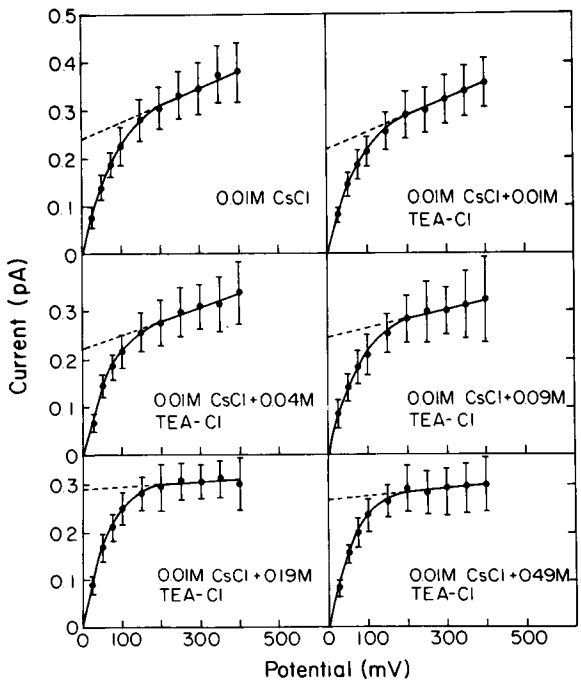


FIGURE 2 Effect of TEACl on the shape of single-channel current-voltage characteristics at a constant CsCl concentration, 0.01 M. The TEACl concentrations are indicated on the graphs. The data points and line segments have the same significance as in Fig. 1.

[3]Independent experimental evidence, that the aqueous double layers function as essentially infinite reservoirs, has been obtained by Apell et al. (1979). These investigators found that the conductance of gramicidin A channels in phosphatidylserine membranes is essentially independent of permeant ion concentration (ionic strength) between 0.01 and 1.0 M CsCl.

age-dependent, almost voltage-independent, limiting behavior at very high applied potentials (300 mV $\leq V \leq$ 500 mV). At lower CsCl concentrations, on the other hand, the asymptotic voltage-dependence of the shapes of the currents at high potential becomes more pronounced. In 0.01 M CsCl the currents vary strongly, albeit linearly, with applied potential (200 mV $\leq V \leq$ 500 mV).

These concentration-dependent changes in the shape of the current-voltage characteristics could reflect some intrinsic concentration dependence of the permeability properties of the channel, or they could reflect the effects of changes in ionic strength. To distinguish between these possibilities, experiments were done at a constant CsCl concentration (0.01 M) in the presence of various concentrations of tetraethylammoniumchloride (TEACl), see Fig. 2. Addition of this impermeant electrolyte to the aqueous phases has pronounced effects upon the shape of gramicidin A single-channel current-voltage characteristics. This is particularly noticeable at high potentials, where an increase in TEACl concentration qualitatively has the same effect as an increase in CsCl concentration. At ionic strengths >0.1 M or so the currents reach an essentially voltage-independent limiting value at potentials larger than 200 mV. Similar results were obtained with other ions, see Fig. 3. The addition of TEACl to the aqueous phases again has a pronounced effect upon the slope of single-channel currents at potentials >200 mV. The average voltage dependence of the currents, as estimated from the slopes, decreases from 0.046 ± 0.012 in 0.01 M salt to 0.0072 ± 0.0055 in 0.01 M salt ± 0.49 M TEACl. The effect of TEACl is a consequence of the increase in ionic strength, because addition of an impermeant nonelectrolyte (e.g., 0.98 M urea) to 0.01 M CsCl has no discernible effect on the shape of the current-voltage characteristics (data not shown).[4] It can thus be concluded that the slopes of the asymptotic current-voltage characteristics vary as a function of the ionic strength, while direct effects of the permeant ion concentration changes are of little significance at these low concentrations.

Ionic strength effects on the shape of the single-channel current-voltage characteristics are most dramatic at high potentials. Similar effects are, however, also seen at lower potentials, as can be inferred by inspection of Fig. 3.

## Concentration Dependence of the Asymptotic Current-Voltage Behavior

The preceding data show that the voltage dependence of gramicidin A single-channel current-voltage characteristics varies as a function of the ionic strength of the aqueous phases. The variations are qualitatively consistent with the notion that interfacial polarization affects the currents. To see if these observations in fact can be accounted for by the interfacial polarization, the results from Figs. 1–3 have been compared with the predictions of Eqs. 14, 23, and 24. The basis for the analysis is that the asymptotic voltage dependence at low permeant ion concentrations approaches zero at high ionic strengths, at least for the most permeant ions: $K^+$, $Rb^+$, $Cs^+$, and $NH_4^+$, see Figs. 2 and 3.

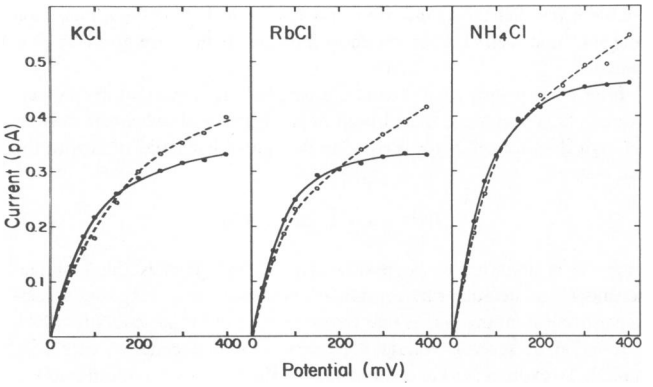


FIGURE 3 The effect of TEACl on the shape of single-channel current-voltage characteristics. The permeant ion concentration was 0.01 M, the permeant ion type is indicated in the graphs. O and --- denote 0.01 M salt; ● and — denote 0.01 M salt + 0.49 M TEACl. The curves have no theoretical significance.

The slope of the current-voltage characteristics at high potentials will in this case be obtained by differentiating Eq. 23 with respect to $u$:

$$\frac{di(u)}{du} = F \cdot k_l^* \cdot c \cdot \alpha + F \cdot c \cdot \left( [1 + \alpha \cdot u] \cdot \frac{dk^*}{du} + k^* \cdot \frac{d\alpha}{du} \right). \quad (25)$$

When $k_l^*$ and $C_m^*$ are voltage-independent (which in this case means that the applied potential does not change the permeability characteristics of the channel or the aqueous convergence regions) Eq. 25 simplifies considerably:

$$\frac{di(u)}{du} = F \cdot k_l^* \cdot c \cdot \alpha = i_{lim} \cdot 2 \cdot kT \cdot A \cdot C_m^*/(e \cdot \sqrt{c_t}) \quad (26)$$

or

$$(1/i_{lim}) \cdot \frac{di(u)}{du} = \alpha = 2 \cdot kT \cdot A \cdot C_m^*/(e \cdot \sqrt{c_t}). \quad (27)$$

Both $[di(u)/du]$ and $i_{lim}$ can be estimated from linear regressions of the single-channel currents at high potentials (the solid lines in Figs. 1 and 2 connect the points used for this analysis).[5] Eqs. 24 and 27 can then be used to obtain estimates for $k_l^*$ and $C_m^*$.

[4]This simple results is only observed at very low permeant ion concentrations. At higher salt concentrations (which for $Cs^+$ means $c \geq 0.1$ M) there are definite effects on the single-channel conductance characteristics when impermeant nonelectrolytes are added to the aqueous phases (Andersen, 1983 *b*; and a manuscript in preparation).

[5]The linear regression procedure cannot be rigorously justified at the lowest ionic strengths because the estimate for $C_m^*$ is so large that Eq. 9 no longer is satisfied. No attempts were, however, made to use more complex fitting functions. I felt that such attempts were unjustified given the shape and standard variations of the data.

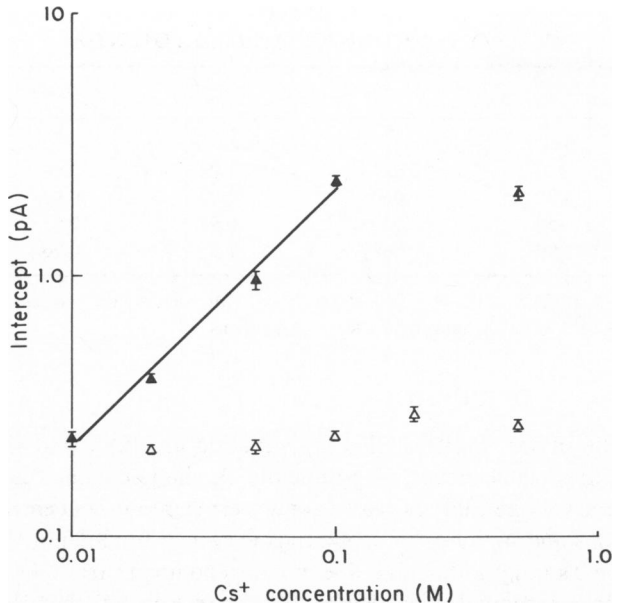


FIGURE 4 Double-logarithmic plot of the current intercepts, determined from the linear regressions in Figs. 1 and 2 (and data in 0.1 M CsCl + 0.4 M TEACl), against the CsCl concentration. ▲ denotes data in pure CsCl; △, data in 0.01 M CsCl + TEACl; ▲ data in 0.1 M CsCl + TEACl. The solid line has a slope of +1.

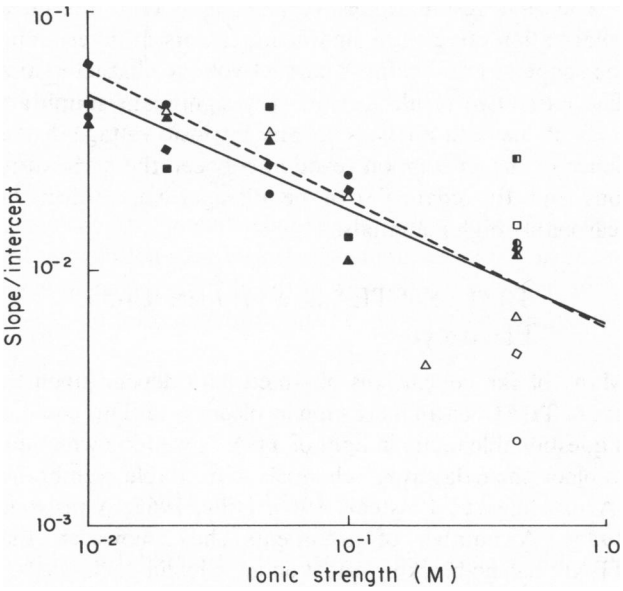


FIGURE 5 Double-logarithmic plot of the slope/intercept from linear regressions of high potential, symptotic single-channel current-voltage characteristics with KCl (■, ◧, □), RbCl (●, ◐, ○), CsCl (▲, ▲, △), and $NH_4Cl$ (◇, ◈, ◆). The filled symbols denote data from experiments in single salt solutions, the half-filled symbols data from experiments in 0.1 M salt + TEACl, the open symbols data from experiments in 0.01 M salt + TEACl. The solid line is determined by least-squares linear regression to the log-transformed data according to Eq. 27. The slope is −0.44, $r = -0.78$. The interrupted line is drawn with a slope of −0.5 using a value of $C_m^* = 1.4\ \mu F/cm^2$.

The results of the linear regression analyses are illustrated in Figs. 4 and 5. Using $Cs^+$ as the permeant ion, one finds that the intercept currents obtained from the linear regressions indeed vary as a linear function of $[Cs^+]$ (Fig. 4). The slopes (normalized by the respective intercepts) on the other hand vary approximately as $1/\sqrt{c_t}$ and the concentration-dependence is similar for $K^+$, $Rb^+$, $Cs^+$, and $NH_4^+$ (Fig. 5). (An equally good $1/\sqrt{c_t}$ dependence was observed when the current intercepts were normalized by $c$ instead of the intercept, data not shown.) It thus seems reasonable to equate the current intercepts with $i_{lim}$, and to use these to obtain estimates for $k_1^*$. These estimates are summarized in Table I. It is likewise possible to estimate $C_m^*$ from the data in Fig. 5, and one finds that $C_m^* = 1.4 \pm 0.8\ \mu F/cm^2$ (the large scatter reflects the difficulty of the measurements and that the estimates of $di(u)/du$ and of $i_{lim}$ are negatively correlated, such that an overestimate of $di(u)/du$ is associated with an underestimate of $i_{lim}$. This latter characteristic implies additionally that the arithmetic mean will overestimate of the true value of $C_m^*$. The geometric mean is less sensitive to this particular problem. It may thus be more appropriate to estimate $C_m^*$ by the geometric mean value: $1.2\ \mu F/cm^2$.) This estimate of $C_m^*$ should be compared with the specific geometric capacitance of unmodified diphytanoylphosphatidylcholine/*n*-decane bilayers, $C_m$, which is $0.45 \pm 0.02\ \mu F/cm^2$ (mean ± SD) in 0.1 M CsCl (Green and Andersen, unpublished observation). This value for the capacitance is larger than that observed in NaCl solutions, $0.4\ \mu F/cm^2$ (Benz and Janko, 1976; Procopio and Andersen, unpublished observations). The reason for the discrepancy is not clear.

The estimate for $C_m^*$ is much higher than the measured values for $C_m$. This result is expected since the channel is more polar than the surrounding bilayer. But this result would also be obtained if the applied potential affects the channel and its immediate surroundings in such a way that either $C_m^*$ or $k_1^*$ increase as a function of the applied potential. Such a voltage-dependent variation in channel properties will, of course, have consequences for the interpretation of the shape of the current-voltage characteristics. It is therefore important that there exists an additional approach to estimate $C_m^*$ that does not depend upon the concentration variations of $di(u)/du$. At a constant applied potential, $u$, but at two different permeant ion concentrations, $c_1$ and $c_2$ (it will for simplicity be assumed that no support electrolyte is present), the ratio of the single-

TABLE I
ESTIMATED VALUES OF $k_1^*$ FOR DIFFERENT CATIONS

| | $K^+$ | $Rb^+$ | $Cs^+$ | $NH_4^+$ |
|---|---|---|---|---|
| *liter/(mol · s)* | | | | |
| $k_1^*$ ($\times 10^{-8}$) | 1.5 | 1.5 | 1.5 | 2.0 |
| SD ($\times 10^{-8}$) | 0.2 | 0.2 | 0.2 | 0.4 |

$0.01M \le c \le 0.1M$; $c_t \le 0.5M$.

channel currents can be expressed as

$$\frac{i(u, c_1) \cdot c_2}{i(u, c_2) \cdot c_1} = \frac{1 + 2 \cdot kT \cdot A \cdot C_m^* \cdot u/(e\sqrt{c_1})}{1 + 2 \cdot kT \cdot A \cdot C_m^* \cdot u/(e\sqrt{c_2})} \quad (28)$$

or

$$\frac{i(u, c_1) \cdot c_2}{i(u, c_2) \cdot c_1} = 1 + \frac{(2 \cdot kT \cdot A \cdot C_m^* \cdot u/e) \cdot (1/\sqrt{c_1} - 1/\sqrt{c_2})}{1 + 2 \cdot kT \cdot A \cdot C_m^* \cdot u/(e\sqrt{c_2})}. \quad (29)$$

At a constant $c_2$, $[i(u, c_1) \cdot c_2]/[i(u, c_2) \cdot c_1]$ should therefore vary as a linear function of $1/\sqrt{c_1}$, with a slope $\alpha'$ given by

$$\alpha' = \frac{2 \cdot kT \cdot A \cdot C_m^* \cdot u}{e + 2 \cdot kT \cdot A \cdot C_m^* \cdot u/\sqrt{c_2}}. \quad (30)$$

The $1/\sqrt{c}$ dependence in Eqs. 28–30 is simply a reflection of the $1/\sqrt{c}$ dependence of $L_D$. Fig. 6 illustrates that the data for KCl, RbCl, CsCl, and $NH_4Cl$ indeed conform to the predictions of Eq. 29. When $V$ = 500 mV ($u$ = 19.5) and $c_2$ = 0.1 M, $\alpha'$ is equal to 0.0699 $M^{-0.5}$ ($r$ = 0.96). According to Eq. 30 one can thus estimate $C_m^*$ to be 1.05 $\mu F/cm^2$. Table II summarizes estimates for $C_m^*$ at potentials ranging from 350 to 500 mV. There is no systematic variation of $C_m^*$ as a function of applied potential. The average value for $C_m^*$ is 1.05 ± 0.05 $\mu F/cm^2$, this estimate compares reasonably well with the estimates based upon the concentration-dependence of $di(u)/du$. The estimates based on Eqs. 29 and 30 should, however, be less dependent on the assumptions made, and thus be more trustworthy.

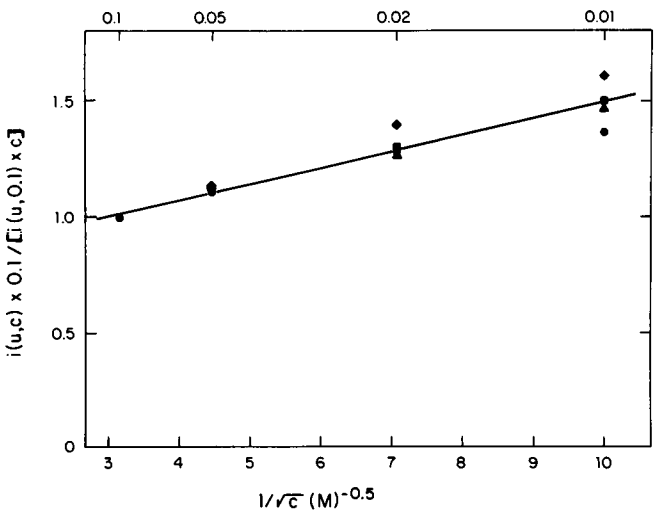


FIGURE 6 Plot of $[i(u,c), 0.1]/[i(u,0.1) \cdot c]$ vs. $1/\sqrt{c}$ for data in KCl (■), RbCl (●), CsCl (▲), and $NH_4Cl$(◆). No impermeant support electrolyte. $u$ = 19.5. The straight line is determined by least-squares linear regression according to Eq. 29. The slope is 0.0699 $M^{-0.5}$; $r$ = 0.96.

TABLE II
$C_m^*$ AS A FUNCTION OF APPLIED POTENTIAL

| $V$ | $\alpha'$ | $C_m^*$ | $r$ |
|---|---|---|---|
| ($mV$) | $M^{-0.5}$ | $\mu F/cm^2$ | |
| 350 | 0.0535 | 1.08 | 0.94 |
| 400 | 0.0600 | 1.08 | 0.97 |
| 450 | 0.0609 | 0.98 | 0.95 |
| 500 | 0.0699 | 1.05 | 0.96 |

KCl, RbCl, CsCl, $NH_4^+Cl$; 0.01 M ≤ $c$ ≤ 0.1M; $r$ denotes the correlation coefficient for the unweighted linear regressions.

## DISCUSSION

The major results of this investigation are first, that the voltage dependence of gramicidin A single-channel current-voltage characteristics at low permeant ion concentrations and high applied potentials vary as a function of the ionic strength, though it does not depend upon variations in the permeant ion concentration per se; second, that this asymptotic voltage dependence, at a constant permeant ion concentration, approaches zero as the ionic strength is increased by addition of an impermeant electrolyte to the aqueous phases; and third, that the applied potentials used here have little or no effect on the intrinsic permeability characteristics of the channels (apart from the usual voltage dependence of the rate constants for ion translocation across any energy barriers that may exist in the translocation path through the channels).

The first result argues very strongly that interfacial polarization effects are significant factors in determining the shape of gramicidin A current-voltage characteristics. The latter two results permit very significant simplifications of the data analysis, as any intrinsic voltage dependence of the association reaction between the permeating ions and the channel can be disregarded, at least at reasonably high potentials.

### The Use of TEA as an Impermeant Electrolyte

Many of the conclusions obtained here depend upon the use of TEACl as an inert support electrolyte. This could be a questionable tactic in light of $TEA^+$'s well-known ability to block the delayed $K^+$ channels in excitable membranes (Armstrong and Binstock, 1965; Hille, 1967; Armstrong, 1975). A number of arguments show, however, that $TEAt^+$ has no blocking effect on gramicidin A channels.

A Priori steric considerations, for example, tend to preclude that $TEA^+$ could block the channel. The gramicidin A channel is generally believed to have fairly uniform luminal dimensions throughout the length of the channel. The luminal radius is ~2 Å (Urry, 1972; see Finkelstein and Andersen, 1981 for functional data supporting this value), while the radius of $TEA^+$, is ~4 Å (Robinson and Stokes, 1965). It is therefore unlikely that $TEA^+$ can enter

and block the channel. It cannot be excluded that $TEA^+$ may be able to adsorb to the channel entrance and thus block the channel.[6] This should be energetically unfavorable, however, considering that the hydrophobic exterior of the $TEA^+$ in this case will interact directly with the very polar peptide moieties lining the channel lumen. It should finally be noted that the smaller, but still impermeable (Hladky and Haydon, 1972), tetramethylammonium ion has similar effects on the shape of the current-voltage characteristics as $TEA^+$ (data not shown).

Experimentally, a voltage-independent block by $TEA^+$ can be excluded because the small-signal conductance, $g$ (25), is essentially unaffected by the addition of $TEA^+$ to the aqueous phases. ($g$ [25] is 3.1 pS in 0.01 M CsCl, decreases to 2.7 pS in 0.01 M CsCl + 0.04 M TEACl, and increases to 3.5 pS in 0.01 M CsCl + 0.49 M TEACl. The conductances variations are small and may reflect changes in ion activity, or changes in surface potential.)[7] A voltage-dependent block by $TEA^+$ can be excluded because there is no evidence for a negative slope resistance at high potentials [see Fig. 2 and 3], not even down to 5 mM Cs [data not shown]. Additional evidence in this regard is provided by the data on $i_{lim}$, because $i_{lim}$ varies linearly with the permeant ion concentration, while there is little variation with changes in the TEACl concentration [Fig. 4]. The small variations in $i_{lim}$ in 0.01 M CsCl + TEACl additions tend to parallel the variations observed for $g$ [25].

There is, therefore, no evidence that $TEA^+$ has any direct effects upon the gramicidin A channel. Neither is there any evidence that the changes in solute concentration by themselves can account for the observed changes in the currents at high potentials. The variations in shape of the current-voltage characteristics that occur upon addition of TEACl to the aqueous phases are, therefore, consequences of the ionic strength changes.

## Interfacial Polarization Effects and the Magnitude of $C_m^*$

The ionic strength dependence of the shape of gramicidin A single-channel current-voltage characteristics suggests strongly that interfacial polarization effects may be important determinants for the shape of the characteristics. This notion is further strengthened by the demonstration that the asymptotic slopes of the current-voltage characteristics (normalized by the respective current intercepts) indeed vary as $1/\sqrt{c_t}$ (Fig. 5) as predicted for interfacial polarization effects (cf. Eqs. 15, 23, and 24). I conclude that the observed asymptotic slopes, and their variations with ionic strength, are the unavoidable results of the interfacial polarization produced by the applied potential.

By analogy with the arguments presented in the preceding article (Andersen, 1983 *a*), it can be shown that the magnitude of the overall rate constant for association of a permeant ion with the gramicidin A channel at sufficiently high potentials becomes controlled by an effectively voltage-independent step. The potential difference necessary to visualize this step depends, of course, on the relative resistances imposed by the association step and the subsequent reactions involved in ion translocation through the channel. This particular element in the association process is most clearly seen with the most permeant ions ($K^+$, $Rb^+$, $Cs^+$, $NH_4^+$, but its existence can also be inferred for $Na^+$, and by extrapolation for $Li^+$ (Andersen, 1983 *a*, *b*).

It is disturbing, of course, that the estimate for $C_m^*$ obtained from this analysis is so much larger than $C_m$, the specific geometric capacitance of unmodified diphytanoylphosphatidylcholine/*n*-decane membranes. It should be noted, however, that a priori arguments suggest that $C_m^*$ should be larger than $C_m$. First, the length of the gramicidin A channel is ~26 Å (Urry, 1972). This is considerably less than the average thickness of the hydrocarbon core of the unmodified bilayer, ~50 Å. The formation of a channel will thus be associated with the formation of a dimple in the bilayer (Haydon, 1975; Neher and Eibl, 1977; Hendry et al., 1978). The local thickness of the channel and its surrounding membrane will be about one-half of the average membrane thickness, and the field in the channel will be twofold larger than the field in the unmodified bilayer. Second, the channel should be more polar than the surrounding hydrocarbon core. Tredgold and Hole (1976) have measured the dielectric constant of dry polypeptides in $\beta$-pleated conformations. They found that the dielectric constant varied between 4 and 25. This will, together with the $H_2O$ present in the channel lumen (Finkelstein, 1974), contribute to make the channel more polar than the surrounding hydrocarbon in the bilayer interior. The increased field and the increased polarity of the channel will both produce an increase in the electric displacement vector **D** at the center of the channel entrance, and thus produce an increased interfacial polarization (Walz et al., 1969).[8]

[6]The helical structure of the gramicidin A channel implies that the channel entrance will be elipsoidal. The dimensions of the entrance will thus exceed those of the lumen itself. Inspection of a Corey-Pauling-Koltun model of the $\beta_6$-helix shows that the dimensions also depend upon the van der Waal's radii of the atoms making up the circumference. The long axis is ~6 Å while the short axis is ~5 Å.

[7]Eisenberg et al. (1979) have shown that the $\xi$-potentials of phospholipid vesicles at a constant ionic strength vary with the cation in the aqueous solution. The $\xi$-potentials are more negative in tetramethylammoniumchloride and TEACl solutions than in solutions containing the chloride salts of the alkali metal cations and $NH_4^+$.

[8]When the interfacial polarization is sufficiently small, so that Eq. 9 holds, $u_{dl}$ should be proportional to the magnitude of **D** at the channel entrance (since the superposition of fields should be a valid procedure). It should thus be possible to characterize the interfacial polarization effects using a phenomenological capacitance $C_m^*$ to describe the dielectric properties of the channel and the surrounding membrane. The relation between $C_m^*$ and the channel properties can, of course, only be approached by exact electrostatic calculations similar to those of Levitt (1978).

The large value of $C^*$ could also reflect that the applied potentials may produce voltage-dependent variations in the channel properties. Such complications must be of minor importance, however. First, the estimates of $C_m^*$ obtained using Eq. 29 do not vary significantly for potentials between 350 and 500 mV (Table II). Electrostrictive effects (changes in membrane thickness) must therefore be of minor importance. Second, at high potentials the single-channel currents become linear functions of potential[9] and the estimate for $C_m^*$ obtained from the ionic strength dependence of the slopes of these line (1.2–1.4 $\mu$F/cm) is in reasonable agreement with the estimates based on the data in Table II (1.05 $\mu$F/cm$^2$). The small difference between the estimates for $C_m^*$ may reflect that $k_\uparrow^*$ varies slightly as a function of potential. These variations must be very small, however, since the single-channel currents become almost completely voltage independent at high TEACl concentrations (Figs. 2 and 3). Additional, more quantitative, support for this argument is provided by estimating the variation in $k_\uparrow^*$ necessary to account for the difference between the two estimates of $C_m^*$. If one assumes that $C_m^*$, and thus $\alpha$, is completely voltage independent, Eq. 25 can be rewritten as

$$\frac{di(u)}{du} = F \cdot k_\uparrow^* \cdot c \cdot \left[\alpha + (1 + \alpha \cdot u) \cdot \frac{d(k_\uparrow^*)}{du}\right]. \qquad (31)$$

Assuming that $C_m^* = 1.05$ $\mu$F/cm, $\alpha$ will vary between 0.0065 in 0.5 M salt and 0.042 in 0.01 M salt. For $u = 15.6$ ($V = 400$ mV), which is the middle of the potential range used to evaluate $di(u)/du$, one finds that $d[\ln(k_\uparrow^*)]/du$ must be somewhere between 0.001 and and 0.009 to account for the difference between the two estimates of $C_m^*$ solely by changes in $k_\uparrow^*$. These estimates of $\alpha$ and $d[\ln(k_\uparrow^*)]/du$ should be compared with the asymptotic voltage dependence of the currents observed in 0.01 and 0.5 M salt, 0.046 and 0.0072, respectively. Because interfacial polarization by necessity must introduce some small voltage dependence of the currents at high potential, it can be concluded that the voltage-variations in ln ($k_\uparrow^*$) must be close to, if not less than, the lower limiting value calculated using Eq. 31. Such small variations in $k_\uparrow^*$, due to direct effects of the applied potential upon the channel structure — possibly mediated by otherwise undetectable membrane thickness changes — or to indirect effects such as changes in the ion distribution in the aqueous convergence/double layer regions, cannot be excluded. These variations must, however, be very small indeed, and they will not be considered further. (Effects due to potential-dependent variations in polar head group orientation or spacing, which could create a voltage-dependent aqueous double layer, seem to be excluded by the finding that TEACl diminishes the voltage dependence of the currents not only in DPPC membranes, but also in GMO membranes [Andersen, 1983 *a*].)

The present results do not in detail address the question of interfacial polarization effects at low potentials, although they exist, see Fig. 3. Analysis of this problem demands more complete information about the kinetics of ion translocation through the channel than is presently available. It seems reasonable, however, to suppose that the value of $C_m^*$ estimated from the data at high potentials reflects some intrinsic, voltage-independent, characteristics of the membrane-bound channel (see also footnote 8), in which case this value for $C_m^*$ should be used to evaluate the significance of interfacial polarization effects at low potentials. But this means that interfacial polarization effects will become more important, and occur at higher ionic strengths, than is usually believed. The basis for the accentuated interfacial polarization is that the magnitude of the interfacial polarization depends upon the ratio $C_m^*/\sqrt{c_t}$ (see Eq. 15). The present value for $C_m^*$ is four times higher than the value used by Walz et al. (1969) to evaluate the importance of interfacial polarization (see their Fig. 3). Interfacial polarization effects are therefore more pronounced, and occur at higher ionic strengths, than predicted in Walz et al.'s original analysis of interfacial polarization effects on current-voltage characteristics in lipid bilayer membranes.

## Consequences of Interfacial Polarization

The importance of interfacial polarization effects extends beyond the shape alterations of the current-voltage characteristics per se. Commensurate changes will occur in the conductance-activity relations. These complications are particularly clearly illustrated for channels occupied by a single permeant ion (for the moment neglecting aqueous diffusion limitations) because the relation between conductance and ion activity in this case ideally should be a simple Langmuir-type saturating function (Läuger, 1973). This simple behavior will, however, change considerably when interfacial polarization effects become important. These complications are best seen by comparing the expressions for the single-channel conductances as a function of potential (see the Appendix for details of the derivation).

In the absence of interfacial polarization the single-channel conductance, $g(u)$, is expressed as

$$g(u) = g_{max}(u) \cdot c/(K(u) + c) \qquad (32)$$

where $g_{max}(u)$ denotes the maximal conductance:

$$g_{max}(u) = \frac{e^2}{kT \cdot u} \cdot \frac{l \cdot k_{-1} \sinh(u/2)}{l \cdot \{\cosh[(\delta_1 + \delta_3) \cdot u] + \cosh[(\delta_1 - \delta_3) \cdot u]\} + k_{-1} \cdot \cosh[(\delta_1 + \delta_2) \cdot u]} \qquad (33)$$

[9]The extent of the linearity is, of course, relative. When the applied potential becomes so large that Eq. 9 no longer applies, the currents should become exponential functions of potential.

such that

$$g_{max}(0) = \frac{e^2}{kT} \cdot \frac{l \cdot k_{-1}}{2 \cdot (2 \cdot l + k_{-1})} \tag{34}$$

and $K(u)$ denotes the concentration (activity) for half-maximal conductance

$$K(u) = \frac{K \cdot (l \cdot \cosh[(\delta_2 + \delta_3) \cdot u] + k_{-1}/2)}{l \cdot \{\cosh[(\delta_1 + \delta_3) \cdot u] + \cosh[(\delta_1 - \delta_3) \cdot u]\} + k_{-1} \cdot \cosh[(\delta_1 + \delta_2) \cdot u]} \tag{35}$$

such that

$$K(0) = K/2 \tag{36}$$

where $K$ is the single-site dissociation constant when $u = 0$ (these expressions follow simply from Eq. A3 when $u_m = u$). Eqs. 32–36 seem more forbidding than they actually are. The content of Eqs. 33 and 34 is that only the rate constant for translocation through the channel interior, $l$, the dissociation rate constant, $k_{-1}$, and the voltage-dependencies ($\delta_3$, $\delta_2$, and $\delta_1$) are relevant for determining the maximal channel conductance at any potential. The content of Eqs. 35 and 36 is that the ion activity for half-maximal conductance is a steady-state characteristic determined by all the rate constants for translocation through the channel and their voltage dependencies.

In the presence of interfacial polarization one can use Eqs. A3, A6, and A7 (see Appendix) to formally write that

$$g(u) = \hat{g}_{max}(u) \cdot c/[\hat{K}(u) + c] \tag{37}$$

where

$$\hat{g}_{max}(u) = \frac{e^2}{kT \cdot u} \cdot \frac{l \cdot k_{-1} \cdot \sinh(u/2)}{l \cdot (\cosh[(\delta_1 + \delta_3 + \delta_2 \cdot 2\alpha) \cdot u] + \cosh\{[\delta_1 - \delta_3 + (\delta_2 + 2 \cdot \delta_3) \cdot 2\alpha]\, u\}) + k_{-1} \cdot \cosh[(\delta_1 + \delta_2 + \delta_3 \cdot 2\alpha) \cdot u]} \tag{38}$$

such that

$$\hat{g}_{max}(0) = \frac{e^2}{kT} \cdot \frac{l \cdot k_{-1}}{2 \cdot (2 \cdot l + k_{-1})} \tag{39}$$

and

$$\hat{K}(u) = \frac{K \cdot (l \cdot \cosh[(\delta_2 + \delta_3) \cdot (l - 2\alpha) \cdot u] + k_{-1}/2)}{l \cdot (\cosh[(\delta_1 + \delta_3 + \delta_2 \cdot 2\alpha) \cdot u] + \cosh\{[\delta_1 - \delta_3 + (\delta_2 + 2 \cdot \delta_3) \cdot 2\alpha]\, u\}) + k_{-1} \cdot \cosh[(\delta_1 + \delta_2 + \delta_3 \cdot 2\alpha) \cdot u]} \tag{40}$$

such that

$$\hat{K}(0) = K/2. \tag{41}$$

Eqs. 37–41 are considerably more complex than Eqs. 32–36, although the general significance of the two sets of equations is similar. The major difference is that Eqs. 38 and 40 also include the effects of having asymmetric ion concentrations at the channel entrance, as well as the difference between $u$ and $u_m$. These are expressed through $\alpha$, but $\alpha$ is a function of $c_i$ (and thus of $c$ unless the experiments are done at a constant ionic strength, it will in the remainder of this section be assumed that $c_i = c$). $\hat{K}(u)$ and $\hat{g}(u)$ will therefore not be constants characterizing the channel; rather, their values will vary with changes in $c$. $\hat{K}(u)$ will generally be $< K(u)$, while the relation between $\hat{g}_{max}(u)$ and $g_{max}(u)$ depends upon the detailed kinetics of ion movement through the channel (see the Appendix).

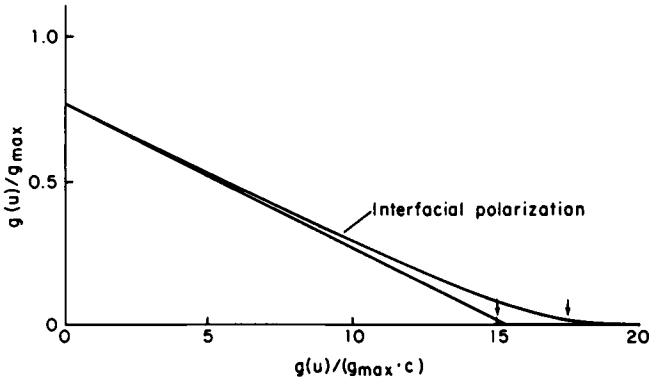


FIGURE 7 Eadie-Hofstee plots of conductance vs. activity data in the absence (straight line) and presence of interfacial polarization. The lines are generated according to Eqs. 32, 33, 35, and Eqs. 37, 38, 40, respectively. The arrows mark the points where $c = 0.001$ M. $K = 0.1$ M; $C_m^* = 1.05\ \mu F/cm^2$; $l/k_{-1} = 100$; $V = 50$ mV. The curvilinear relation will become indistinguishable from the straight line at ionic strengths >0.2 M or so.

The complications induced by interfacial polarization are best illustrated using Eadie-Hofstee plots, see Fig. 7. The straight line denotes the picture expected for a singly occupied channel in the absence of interfacial polarization, while the curvilinear relation is that obtained in the presence of interfacial polarization. The shape of the curve with interfacial polarization effects included is qualitatively similar to the type of curves that generally are

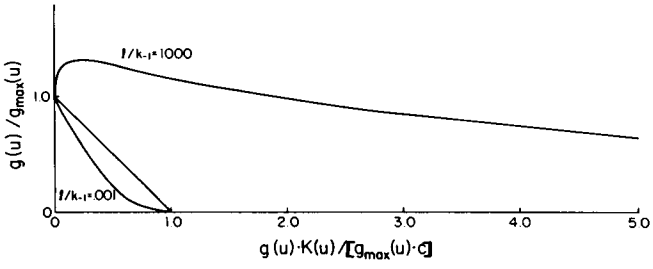


FIGURE 8 Eadie-Hofstee plots of conductance vs. activity in the absence (straight line) and presence of interfacial polarization. The curves are generated according to Eqs. 32, 33, 35, and Eqs. 37, 38, 40, respectively. $K = 0.001$ M; $C_m^* = 1.05\ \mu F/cm^2$; $V = 200$ mV. The numbers adjacent to the curvilinear relations are the values for $l/k_{-1}$ used to generate the plots.

considered to indicate that there are several nonequivalent binding sites for ligand (ion) binding (Edsall and Wyman, 1958; Cantor and Schimmel, 1980). It is thus possible to misinterpret the physical basis for curvilinear Eadie-Hofstee plots observed at low permeant ion concentrations, and erroneously assign the "foot" in the plot to be an indication of multiple ion occupancy in the channel.[10] This problem becomes particularly acute when the Eadie-Hofstee plot not only exhibits a biphasic behavior in the low conductance region, but also a conductance maximum at higher conductances, see Fig. 8. This type of behavior is best seen when $\delta_3$ is close 0.5, $l/k_{-1} >> 1$, and $K$ is sufficiently low ($\leq$ 0.01 M) that the ionic strength can be high vis-a-vis ion occupany while still low enough that interfacial polarization effects produce significant distortions of the conductance vs. activity relation. $\hat{g}_{max}(u)$ can under such circumstances theoretically reach a value equal to $2 \cdot g_{max}(u)$. This limiting behavior is only approached under rather extreme conditions ($\delta_3 = 0.5$, very high applied potentials and very low values for $K$ and $c$). Note, however, that the expression of interfacial polarization is very dependent upon the detailed kinetics of ion movement through the channel. When $l/k_{-1} << 1$, one obtains a very different pattern of distortions than when $l/k_{-1} >> 1$, (Fig. 8). The conditions chosen for generating Fig. 8 are admittedly rather extreme, but the general features of this figure are observed equally well with more conventional choices of $l/k_{-1}$, $K$, and potential (data not shown).

Qualitatively similar distortions in conductance vs. activity relations, and thus in Eadie-Hofstee plots, are observed when double-occupancy models are investigated for interfacial polarization effects (data not shown). The magnitudes and directions of the distortions are again dependent upon the detailed kinetics of ion movement through the channels. It is, therefore, not possible to state to what extent a particular set of measurements may have been contaminated by these problems. The magnitude of the effects is large enough, however, that they should be considered as possible sources of systematic error in single-channel current measurements below 0.1 M or so. The analysis of such data, by fitting theoretical conductance expressions to the data and extracting values for rate cs.tants and dissociation constants, is therefore subject to considerable uncertainties. These uncertainties extend not only to questions about the significance of the values deduced for the various rate constants but, even more serious, to questions about whether the model employed for the analysis is appropriate (interfacial polarization effects are in some respects indistinguishable from the effects of having additional binding sites incorporated into the kinetic model, see footnote 10). These questions may not be too serious for purely kinetic descriptions of ion translocation through the channel. But these problems become disastrous for any attempts to understand the permeability characteristics of the channel in terms of its structural and dynamic characteristics.

[10]It is, at this point, important to distinguish between, on the one hand, the binding of ions into the channel, and the number of physical binding sites that can simultaneously be both associated with the channel entity and occupied, and on the other hand, the number of sites used in the construction of a kinetic model for ion translocation through the channel. The two-site-one-ion model used here is, when interfacial polarization effects are important, in many respects equivalent to a four-site, threeion model in which the outer binding sites (the interfacial regions) are in equilibrium with the bulk aqueous phases and have a low affinity for the permeant ions (so that saturation phenomena are unimportant). Interfacial polarization effects may thus provide a physical basis for the outer binding sites that Eisenman et al. (1980) find to be essential requirements for a successful kinetic description of ion translocation through the gramicidin A channel. Note, however, that the outer binding sites that mimic interfacial polarization effects are bookkeeping devices in the sense that there is no structural basis for their existence. These outer binding sites appear only as intermediary steps in the equations describing the ion movement through the channel. They would not appear in equilibrium binding studies of the channel.

## APPENDIX

## Interfacial Polarization Effects in a Two-Site-One-Ion Channel

The model is similar to that used in Andersen (1983 *a*). It is assumed that the channel contains two major free-energy minima (the ion binding sites) and that these are separated from each other and from the aqueous phases by energy barriers. It is further assumed that ion movement through the channel can be subdivided into three distinct steps corresponding to the association reaction, the translocation through the channel interior, and the dissociation reaction, respectively:

$$I' + G \underset{k''_{-1}}{\overset{k'_1}{\rightleftharpoons}} IG \underset{l''}{\overset{l'}{\rightleftharpoons}} GI \underset{k''_1}{\overset{k'_{-1}}{\rightleftharpoons}} G + I'' \qquad \text{(A1)}$$

$I'$ and $I''$ represents an ion at the left and right channel entrances, respectively, $G$, $IG$, and $GI$ denotes a channel without ions, or with an ion in the left or the right free energy minimum. The rate constants for crossing each barrier are denoted by the lower case letters, the superscripts $'$ and $''$ denote that their magnitudes will be biased by the applied potential. The same superscripts are used to account for the voltage-dependent variation in ion concentrations.

The single-channel current is:

$$i(u) = \frac{e \cdot (k'_1 \cdot l' \cdot k'_{-1} \cdot c' - k''_1 \cdot l'' \cdot k''_{-1} \cdot c'')}{(k'_{-1} \cdot k''_{-1} + l' \cdot k'_{-1} + l'' \cdot k''_{-1}) + k'_1 \cdot c'(l' + l'' + k'_{-1}) + k''_1 \cdot c'' \cdot (l' + l'' + k''_{-1})} \qquad \text{(A2)}$$

The distribution of the applied potential difference across the channel and its adjacent aqueous double layers is given by Eqs. 3–5, and the ion concentrations at the channel entrances, $c'$ and $c''$, are given by Eqs. 10 and 13. If it is assumed that the energy barriers are sharp enough that the rate constants are exponential functions of the potential difference between an energy well (or the aqueous phase) and the adjacent barrier peak then the current can be expressed as

$$i(u) = \frac{e \cdot l \cdot k_{-1} \cdot c \cdot \sinh(u/2)}{K \cdot \{l \cdot \cosh[(\delta_2 + \delta_3) \cdot u_m] + k_{-1}/2\} + c \cdot (l \cdot \{\cosh[(\delta_1 + \delta_3) \cdot u_m + u_{dl}] + \cosh[(\delta_1 - \delta_3) \cdot u_m + u_{dl}]\} + k_{-1} \cdot \cosh[(\delta_1 + \delta_2) \cdot u_m + u_{dl}])} \qquad \text{(A3)}$$

where $K = k_{-1}/k_1$, $u_m = V_m \cdot e/kT$ and $\delta_1$, $\delta_2$, and $\delta_3$ denote the fraction of $u$ that affects $k_1$, $k_{-1}$, and $l$, respectively. (Note that Eq. A3 reverts into

Eq. A4 of Andersen (1982 *a*) if the outer barriers are symmetrical and $\delta = 2 \cdot \delta_3$).

Two limiting expressions of Eq. A3 are of interest, namely the expression for $i(u)$ when $c << K$ (when the channel has a very low probability of being occupied) and the expression for $i(u)$ when $c >> K$ (when the channel is fully occupied). In the former case Eq. A3 simplifies to

$$i(u) = \frac{e \cdot k_1 \cdot c \cdot l \cdot \sinh(u/2)}{l \cdot \cosh[(\delta_2 + \delta_3) \cdot u_m] + k_{-1}/2} \quad \text{(A4)}$$

which describes how the expression of interfacial polarization effects varies as a function of the detailed kinetics of ion translocation through the channel. When the major barrier for ion movement through the channel is the translocation step through the channel interior (when $l << k_{-1}$) interfacial polarization will not express itself as long as $u << \operatorname{arccosh}(k_{-1}/2 \cdot l)/(\delta_2 + \delta_3)$. This somewhat paradoxical result occurs because the decrease in transmembrane potential ($u_m$) is exactly balanced by the changes in interfacial ion concentrations. On the other hand, when the major barrier is the exit step (when $k_{-1} << l$), one finds that interfacial polarization effects are most pronounced and observable at all potentials. The apparent voltage dependence $\delta_1'$ of $k_1'$ is in this case equal to $[\delta_1 \cdot (1 - 2\alpha) + \alpha]$. Fig. 9 illustrates how the expression of interfacial polarization varies as a function of $l/k_{-1}$ when $c = 0.01$ or 0.1 M and $\delta_1 = 0$ (even more pronounced effects will, of course, be seen at lower salt concentrations).

The other limiting case occurs when $c >> K$ and $c$ is sufficiently low that interfacial polarization effects are important. In this situation Eq. A3 reduces to

$$i(u) = \frac{e \cdot l \cdot k_{-1} \cdot \sinh(u/2)}{l \cdot \{\cosh[(\delta_1 + \delta_3) \cdot u_m + u_{dl}] + \cosh[(\delta_1 - \delta_3) \cdot u_m + u_{dl}]\} + k_{-1} \cdot \cosh[(\delta_1 + \delta_2) \cdot u_m + u_{dl}]}. \quad \text{(A5)}$$

Note that even though $c$ does not appear explicitly, then there is a dependence upon $c$ through $u_m$ and $u_{dl}$. More detailed analysis of interfacial polarization effects under these circumstances are best pursued by writing $u_m$ and $u_{dl}$ as

$$u_m = (1 - 2\alpha) \cdot u \quad \text{(A6)}$$

and

$$u_{dl} = \alpha \cdot u \quad \text{(A7)}$$

and insert these expressions into Eq. A5 to give

$$i(u) = \frac{e \cdot l \cdot k_{-1} \cdot \sinh(u/2)}{l \cdot (\cosh[(\delta_1 + \delta_3 + \delta_2 \cdot 2\alpha) \cdot u] + \cosh\{[\delta_1 - \delta_3 + (\delta_2 + 2 \cdot \delta_3)\, 2\alpha]u\}) + k_{-1} \cdot \cosh[(\delta_1 + \delta_2 + \delta_3 \cdot 2\alpha)u]}. \quad \text{(A8)}$$

Inspection of Eq. A8 shows how the expression of interfacial polarization effects in this limit depends upon the detailed kinetics of ion translocation through the channel. A complete analysis of the behavior Eq. A8 under different conditions is therefore quite tedious, albeit straightforward, and will not be pursued here. Fig. 10 illustrates, however, the general patterns observed, in particular how the shape changes depend upon the values of $l/k_{-1}$ as well as $\delta_1$, $\delta_2$, $\delta_3$. It should be noted that the currents at very high potentials generally will be less than in the absence of interfacial polarization. This rather unexpected result arises because the major interfacial polarization effect will be the reduction of the potential across the channel. The shift in ion distribution in the channel, brought about by the changes in interfacial ion concentrations, will generally not be able to compensate for the decrease in $u$. The exceptions to this pattern occur when $\delta_1 = 0$ (and $\delta_2 < \delta_3$) or when $\delta_2 = 0$ (and $\delta_1 < \delta_3$) particularly when

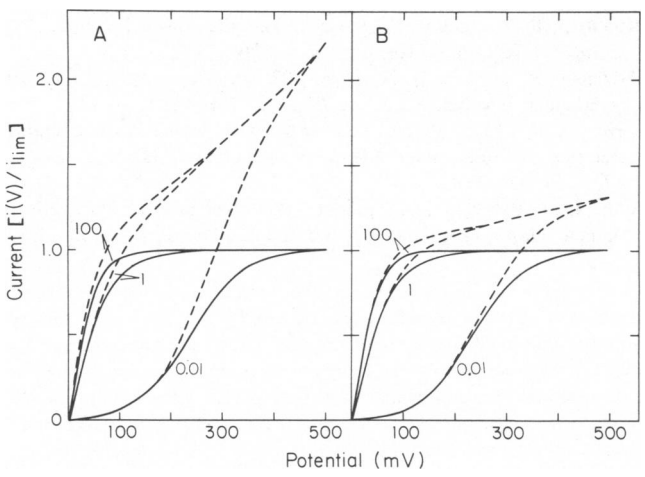


FIGURE 9 Current-voltage characteristics at low channel occupancy in the absence and presence of interfacial polarization effects. The curves are generated according to Eq. A4. The currents are normalized by $i_{lim}$. (*A*) $c = 0.01$ M; (*B*) $c = 0.1$ M. $\delta_1 = 0$. The solid lines denote the pattern seen in the absence of interfacial polarization ($u_m = u$, $u_{dl} = 0$), the interrupted lines denote the pattern seen in the presence of interfacial polarization, $C_m' = 1.05\ \mu F/cm^2$. The numbers adjacent to the curves indicate the values of $l/k_{-1}$.

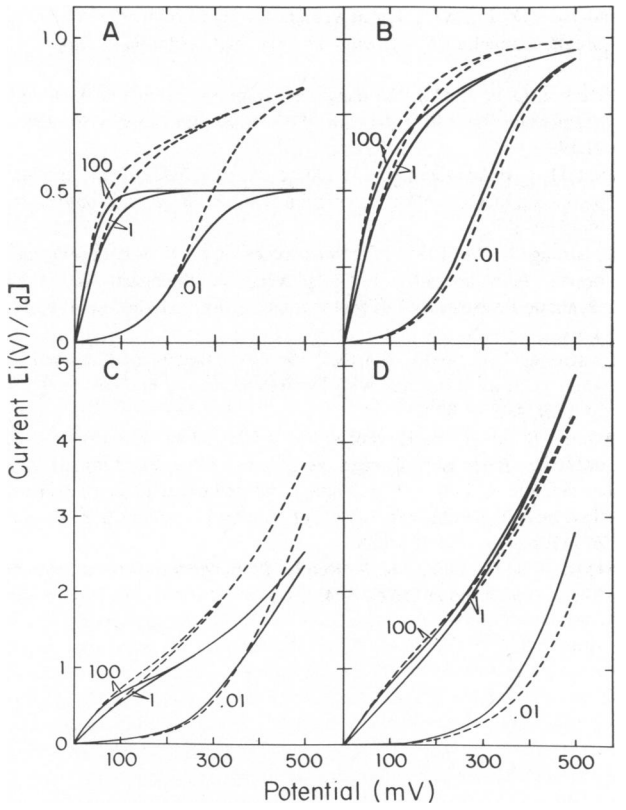


FIGURE 10 Current-voltage characteristics at high channel occupancy in the absence and presence of interfacial polarization effects. The curves are generated according to Eq. A8, $c_t = 0.01$ M. (*A*) $\delta_1 = \delta_2 = 0$, $\delta_3 = 0.5$; (*B*) $\delta_1 = 0.08333$, $\delta_2 = 0$, $\delta_3 = 0.41667$; (*C*) $\delta_1 = 0$, $\delta_2 = 0.08333$, $\delta_3 = 0.41667$; (*D*) $\delta_1 = \delta_2 = 0.08333$, $\delta_3 = 0.3334$. The currents are normalized by $i_d = e \cdot k_{-1}$. The solid lines show the pattern seen in the absence of interfacial polarization, $\alpha = 0$; the interrupted lines show the pattern seen in the presence of interfacial polarization, $C_m' = 1.05\ \mu F/cm$. The numbers adjacent to the curves indicate the values of $l/k_{-1}$.

both $\delta_1$ and $\delta_2$ are zero (or $\delta_3 = 0.5$) in which case the current in the presence of interfacial polarization reaches a value that is twice that observed in the absence of these complications (as may inferred from Fig. 10 *A*). These occupancy-dependent interfacial polarization effects on the current-voltage characteristics will also be reflected in the conductance vs. activity characteristics of membrane-bound channels, particularly at higher potentials (this case $V \geq 25$ mV). The interpretation of conductance data as a function of permeant ion activity will thus be compromised by these problems and be much less definitive than generally assumed. Some of the complexities that may be encountered in these analyses are illustrated in Figs. 7 and 8 (see Discussion).

I would like to thank S. W. Feldberg, R. Muller, and O. Sten-Knudsen for discussions and helpful criticism of a previous version of this manuscript.

This work was supported by National Institutes of Health grant GM 21342, by a New York Heart Association Senior Investigator Award, and by an Irma T. Hirschl Career-Scientist Award.

*Received for publication 16 October 1981 and in revised form 29 September 1982.*

## REFERENCES

Andersen, O. S. 1983 *a*. Ion movement through gramicidin A channels. Single-channel measurements at very high potentials. *Biophys. J.* 41:119–133.

Andersen, O. S. 1983 *b*. Ion movement through gramicidin A channels. Studies on the diffusion-controlled association step. *Biophys. J.* 41:147–165.

Apell, H. J., E. Bamberg, and P. Läuger. 1979. Effects of surface charge on the conductance of the gramicidin channel. *Biochim. Biophys. Acta.* 552:369–378.

Armstrong, C. M. 1975. Potassium pores of nerve and muscle membranes. *In* Membranes. Lipid Bilayers and Biological Membranes: Dynamic Properties. G. Eisenman, editor. Marcel Dekker, Inc., New York. 3:325–358.

Armstrong, C. M., and L. Binstock. 1965. Anomalous rectification in the squid giant axon injected with tetraethylammonium chloride. *J. Gen. Physiol.* 48:859–872.

Aveyard, R., and D. A. Haydon. 1973. An Introduction to the Principles of Surface Chemistry. Cambridge University Press, London. 31–57.

Benz, R., and K. Janko. 1976. Voltage-induced capacitance relaxation of lipid bilayer membranes. Effects of membrane composition. *Biochim. Biophys. Acta.* 455:721–738.

Bockris, J. O. M., and A. K. N. Reddy. 1970. Modern Electrochemistry. Macdonald, London. 2:623–844.

Cantor, C. R., and P. R. Schimmel. 1980. Biophysical Chemistry, part III. W. H. Freeman & Company, Publishers, San Francisco. 849–886.

Edsall, J. T., and J. Wyman. 1958. Biophysical Chemistry. Vol. I. Academic Press, Inc., New York. 591–662.

Eisenberg, M., T. Gresalfi, T. Riccio, and S. McLaughlin. 1979. The adsorption of monovalent cations to bilayer membranes containing negative phospholipids. *Biochemistry.* 18:5213–5223.

Eisenman, G., J. Hägglund, J. Sandblom, and B. Enos. 1980. The current-voltage behavior of ion channels: important features of the energy profile of the gramicidin channel deduced from the conductance-voltage characteristics in the limit of low ion concentrations. *Ups. J. Med. Sci.* 85:247–257.

Everitt, C. T., and D. A. Haydon. 1968. Electrical capacitance of a lipid membrane separating two aqueous phases. *J. Theoret. Biol.* 18:371–379.

Finkelstein, A. 1974. Aqueous pores created in thin lipid membranes by the antibiotics hystatin, amphotericin B, and gramicidin A: implications for pores in plasma membranes. *In* Drugs and Transport Processes. B. A. Callingham, editor. The McMillan Press, Ltd., London. 241–250.

Finkelstein, A., and O. S. Andersen. 1981. The gramicidin A channel: a review of its permeability characteristics with special reference to the single-file aspect of transport. *J. Membr. Biol.* 59:155–171.

Haydon, D. A. 1975. Functions of the lipid in bilayer ion permeability. *Ann. N. Y. Acad. Sci.* 264:2–16.

Hendry, B. M., B. W. Urban, and D. A. Haydon. 1978. The blockage of the electrical conductance in a pore-containing membrane by the *n*-alkanes. *Biochim. Biophys. Acta.* 513:106–116.

Hille, B. 1967. The selective inhibition of delayed potassium currents in nerve by tetraethylammonium ion. *J. Gen. Physiol.* 50:1287–1302.

Hladky, S. B., and D. A. Haydon. 1972. Ion transfer across lipid membranes in the presence of gramicidin A. Studies of the unit conductance channel. *Biochim. Biophys. Acta.* 274:294–312.

Läuger, P. 1973. Ion transport through pores: a rate-theory analysis. *Biochim. Biophys. Acta.* 311:423–441.

Levitt, D. G. 1978. Electrostatic calculations for an ion channel. I. Energy and potential profiles and interactions between ions. *Biophys. J.* 22:209–219.

Neher, E., and H.-J. Eibl. 1977. The influence of phospholipid polar groups on gramicidin channels. *Biochim. Biophys. Acta.* 464:37–44.

Robinson, R. A., and R. H. Stokes. 1965. Electrolyte Solutions. 2nd edition, revised. Butterworths, London. 120–125.

Tredgold, R. H., and P. N. Hole. 1976. Dielectric behavior of dry synthetic polypeptides. *Biochim. Biophys. Acta.* 443:137–142.

Urry, D. W. 1972. Protein conformation in biomembranes: optical rotation and absorption of membrane suspensions. *Biochim. Biophys. Acta.* 265:115–168.

Walz, D., E. Bamberg, and P. Läuger. 1969. Nonlinear electrical effects in lipid bilayer membranes. I. Ion injection. *Biophys. J.* 9:1150–1159.